

# SYNCHROTRON RADIATION BEAM DIAGNOSTICS FOR THE INTEGRABLE OPTICS TEST ACCELERATOR\*

N. Kuklev<sup>†</sup>, Y.-K. Kim, University of Chicago, Chicago, IL 60637, USA  
A. L. Romanov, Fermilab, Batavia, IL 60510, USA

## Abstract

The Integrable Optics Test Accelerator (IOTA) is a research electron and proton storage ring currently being commissioned at Fermilab's Accelerator Science and Technology (FAST) facility. An extensive beam physics research program is planned, including tests of novel techniques for improving beam intensity, stability, and emittance. A key part of IOTA beam diagnostics suite are synchrotron light beam monitors, mounted onto each dipole. In this paper, we present the hardware and software design of this system. Mechanical layout and actuator control electronics are described. High throughput image acquisition and analysis architecture is outlined, and its preliminary performance is explored. Integration of the system within accelerator control network and possible user applications, such as camera auto-focusing, are discussed.

## INTRODUCTION

Integrable Optics Test Accelerator (IOTA) is a research electron and proton storage ring currently undergoing final assembly and commissioning at Fermilab's Accelerator Science and Technology (FAST) facility. It has a circumference of 40m, and is designed to use either 2.5 MeV protons provided by an RFQ injector, or 150 MeV electrons from FAST linac [1]. A wide variety of experiments are planned, including a demonstration of optical stochastic cooling [2, 3] as well as techniques for improving proton beam intensity and stability - electron lenses and quasi-integrable optics [4], the latter using strongly nonlinear magnetic inserts placed in special equal beta function drift regions, as shown on ring schematic in Fig. 1.

During first season, system will be run exclusively with electron beams which will be used as a macroparticle to probe dynamics in the studied systems for all physically available amplitudes. For this process, a large suite of beam diagnostic systems will be used, including scintillation screens, wall current monitors, faraday cups (in linac), as well as electrostatic beam position monitors (BPMs), and synchrotron light (SL, SyncLight) cameras. The latter will provide unique, non-destructive measurements of beam profile, as well as position and intensity.

## SYSTEM OVERVIEW

Synchrotron radiation (SR) is produced by charged particles undergoing radial acceleration, a byproduct in any

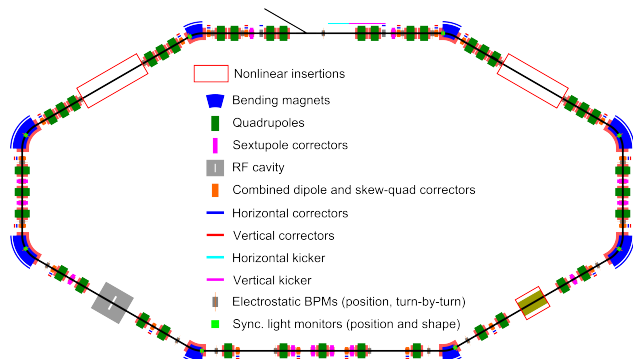


Figure 1: Layout of IOTA ring, with electron and proton injection in the upper central section.

storage ring. It plays a large role in beam damping, and is also a commonly used diagnostic signal [5, 6]. SR intensity profile is strongly forward peaked, with total radiation power scaling as fourth power of particle energy. Unfortunately, 2.5 MeV protons, due to their high mass, do not produce sufficiently intense or energetic SR signal, and as such, IOTA SyncLight system is intended exclusively for electron beam operation. Its main design requirements are to resolve beam features with sufficient spatial resolution ( $\approx 10\text{-}15\ \mu\text{m}$ ) and update frequency (above 10 Hz), with each parameter imposing unique challenges on hardware and software. Additionally, due to time and difficulty in accessing IOTA during operation, a complete remote control capability is necessary, while keeping per-detector costs reasonable and allowing for easy future additions.

## Hardware Design

IOTA ring contains 8 bending dipole magnets, with 4 each of 30 and 60 degree varieties. Vacuum chambers for each type were designed with additional window ports, allowing for emitted SR to be extracted from beam line downstream of the magnet. A simple enclosed optical system, rigidly mounted via an extruded aluminum frame, is then used to focus and steer SR towards a camera, as shown for 30 degree magnet in Fig. 2. It is comprised of several standard optical components - two steerable mirror mounts with a diaphragm collimator, color and neutral density filters, and a 400-700 nm doublet lens positioned at appropriate path length. This allows image formation with minimized impact from chromatic aberrations, diffraction, and depth of field effects, while keeping overall system simple and relatively cheap. A commercial off the shelf PointGrey BlackFly 23S6M camera mounted on a precision linear stage is used as a monochromatic detector, with pixel size of  $5.86\ \mu\text{m}$

\* Work supported by the U.S. National Science Foundation under Award PHY-1535639. Fermi Research Alliance, LLC operates Fermilab under Contract DE-AC02-07CH11359 with the US Department of Energy.

<sup>†</sup> nkuklev@uchicago.edu

Content from this work may be used under the terms of the CC BY 3.0 licence (© 2018). Any distribution of this work must maintain attribution to the author(s), title of the work, publisher, and DOI.

and 0.837 optical magnification resulting in 7  $\mu\text{m}$  nominal resolution. Green light (525nm) band was chosen as operating point due to maximum product of detector quantum efficiency and SR intensity, while having acceptable optical errors.

To allow for automatic operation, three motorized open-loop controlled axes are installed - two for mirror steering (transverse to the beam), and one for camera focus (along the beam). For the step angle and stage used, a nominal repeatability of under 3  $\mu\text{m}$  is expected on each axis, significantly below other positioning errors and imperfections in the system. The motors are powered through a custom-designed 3 channel stepper driver PCB that is interfaced with a RaspberryPi 3B (RasPi) control node via a GPIO interface. A set of redundant limit switches is used to ensure soft and hard limits on all motions as well as to provide homing functionality. Power and control signals are transferred over PoE-enabled ethernet cables to both camera and RasPi node, with a separate high voltage line to stepper motors, all enclosed in appropriate shielding and feedthroughs. Control electronics are separated into a dedicated enclosure, allowing service access without disturbing the optics. A number of spare channels were left unpopulated to allow for future extensions of the system, such as addition of photo-multiplier tubes (PMTs) and motorized filter wheels.

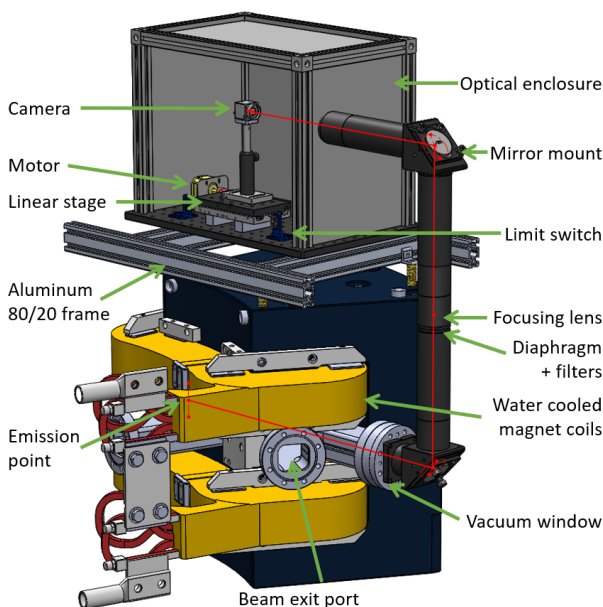


Figure 2: CAD model with optical path trace (red). Two ports are evident, with beamline exit on the left and SR output on the right. Light emission occurs at magnet entrance.

### Software Architecture

To enable live image processing at peak rate of 1Gb/s (up to 40FPS, <25ms max processing time), DAQ functionality was isolated from other tasks, resulting in two loosely coupled subsystems, the architecture of which is shown in Fig. 3. For image DAQ, a high performance C++/Python

code was written to quickly extract key beam parameters - position, profile, and peak/total intensity, via an optimized 2D Gaussian curve fit routine, with region of interest and noise rejection/background subtraction preprocessing. This algorithm, with appropriate initial parameter guesses based on data moments, was effective for simulated near-Gaussian beams, and more algorithms are in development to deal with irregular beam shapes. Once extracted, beam parameters are then forwarded to a common BPM server that handles data aggregation from various sources, and communicates with custom clients and Fermilab's Accelerator Control NETWORK (ACNET), a laboratory-wide control system responsible for running all major parts of IOTA.

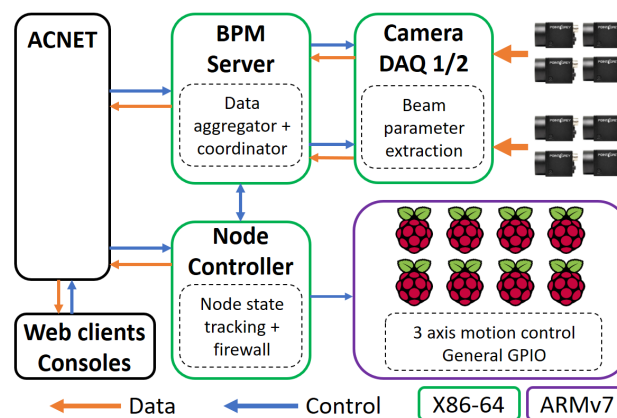


Figure 3: Software architecture overview.

For node control, a separate software stack was written in python 3, with some C/C++ hot loop optimization. It is comprised of two node types - isolated worker nodes themselves (RasPi, ARM), as well as a control node (x86 server) responsible for outward facing communication, state tracking, and setting up worker nodes via Ansible configuration management framework. While providing the convenience and flexibility of a complete Linux OS, systems like RaspberryPi are generally unsuitable for real-time tasks. An extensive modification and setup of worker nodes was undertaken to optimize for direct motor control, including real-time kernel patches and control thread core isolation. These allowed for sufficient GPIO timing (5  $\mu\text{s}$  jitter) and interrupt handling (80  $\mu\text{s}$  latency) performance, avoiding microcontroller intermediaries and simplifying the overall design. Extensive logging and auditing system on the control node, with periodic worker log sync, was added to aid in quick, remote debugging. In addition, safety interlocks, and hardware temperature and undervoltage fault monitoring was incorporated to ensure fail-safe operation.

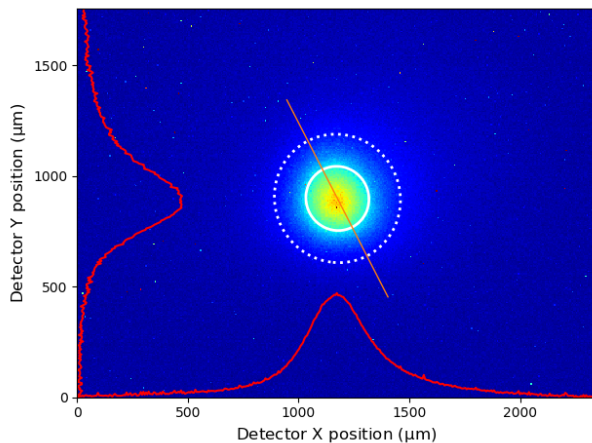
### PROTOTYPE ASSEMBLY AND TESTING

In preparation for serial production, a standalone test system was assembled, as shown in Fig. 4a. No significant design deficiencies were identified, with good optical alignment and structural rigidity. To test optical performance, a modified monochromatic LED light source was used to

simulate a typical beam, with overlaid pinpoint aperture producing an approximately Gaussian profile at intensities comparable to operational ones. The collected images, example of which is shown in Fig. 4b, were fitted with analysis algorithm described above, finding expected near-Gaussian shape and an average FWHM of  $360\ \mu\text{m}$ . While slightly larger than beam sizes expected during actual operation ( $100\text{--}200\ \mu\text{m}$ ), that was still well within region of interest.



(a) Prototype mounted on 60 degree magnet



(b) Beam simulator profile, with 2D Gaussian fit and projections. Solid/dotted contours denote  $1\sigma/2\sigma$ , orange line major semiaxis.

Figure 4: Prototype assembly and test results

As a validation experiment and demonstration of user application network control, this light source was used for a focal point search, one of key calibration processes for actual beam measurements. It is performed by moving the stage through a full range of motion, sampling and fitting beam profiles at each step. The resulting beam parameter series are then fitted with expected Gaussian optics scaling relations to find optimal focal positions. Results from a representative automated 23 position, 79 image run (execution time 89s) are shown in Fig. 5. All three parameter fits, although simplistic, can be seen to reliably find the best position to within  $500\ \mu\text{m}$ , with near-perfect model agreement. More advanced fitting

routines and focus algorithms are expected to improve this result.

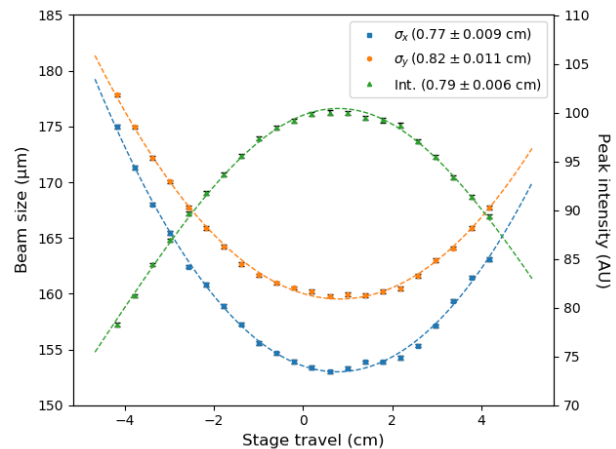


Figure 5: Beam parameter fits with optimal focus positions.

## SUMMARY AND FUTURE WORK

We have presented a hardware and software design of SR beam diagnostic system for the IOTA storage ring, as well as promising preliminary results from a standalone prototype. Serial station construction is on track to begin in early summer, with commissioning soon to follow. Based on current results, our system is expected to meet all design and budgetary requirements.

Various additions are currently under consideration, including addition of low light PMT-based detectors for turn-by-turn data and single electron experiments, as well as more advanced multi-pixel PMT systems. We expect that these can be accommodated with minimal modification to base design.

## ACKNOWLEDGEMENTS

The authors wish to thank J. Santucci, M. Obrycki, B. Hartsell (FNAL), R. Northrop (UChicago), as well other support staff for their help in design, procurement, and assembly. We are also grateful to A. Valishev for his advice and discussions.

## REFERENCES

- [1] S. Antipov *et al.*, “IOTA (Integrable Optics Test Accelerator): facility and experimental beam physics program,” *J. Instrum.*, vol. 12, no. 03, T03002, 2017, <http://stacks.iop.org/1748-0221/12/i=03/a=T03002>
- [2] V. Lebedev, “Optical Stochastic Cooling,” *ICFA Beam Dyn. Newslett.*, vol. 65, pp. 100–116, 2014.
- [3] Y. S. Derbenev, “Theory of electron cooling,” 2017, [arXiv:1703.09735](https://arxiv.org/abs/1703.09735)
- [4] V. Danilov and S. Nagaitsev, “Nonlinear accelerator lattices with one and two analytic invariants,” *Phys. Rev. ST Accel. Beams*, vol. 13, p. 084002, 2010, doi:10.1103/PhysRevSTAB.13.084002

Content from this work may be used under the terms of the CC BY 3.0 licence (© 2018). Any distribution of this work must maintain attribution to the author(s), title of the work, publisher, and DOI.

- [5] R. Thurman-Keup *et al.*, “Synchrotron radiation based beam diagnostics at the fermilab tevatron,” *J. Instrum.*, vol. 6, no. 09, T09003, 2011, <http://stacks.iop.org/1748-0221/6/i=09/a=T09003>
- [6] R. Jung, P. Komorowski, L. Ponce, and D. Tommasini, “The LHC 450-GeV to 7-TeV synchrotron radiation profile monitor using a superconducting undulator,” in *Proc. AIP Conf.*, vol. 648, pp. 220–228, 2003, doi:10.1063/1.1524404